Calorimetric and Molecular Orbital Studies of Hydrogen Bonding between Hydrogen Fluoride and Cyclic Ethers

Mitsunori Tsuda,[1a] Hidekazu Touhara,[1a] Koichiro Nakanishi,*[1a] Kazuo Kitaura,[1b] and Keiji Morokuma[1b]

Contribution from the Department of Industrial Chemistry, Kyoto University, Kyoto 606, Japan, and Institute for Molecular Science, Myodaiji, Okazaki 444, Japan. Received May 8, 1978

Abstract: The enthalpies of formation of hydrogen bonding complexes $\Delta H°$ were obtained by precision calorimetry for hydrogen fluoride (HF)–furan, HF–tetrahydrofuran (THF), HF–2,5-dimethylfuran (2,5-di-MeF), and HF–2,5-dimethyltetrahydrofuran (2,5-di-MeTHF). The frequency shift $\Delta\nu_{HF}$ of H–F stretching vibration due to hydrogen bond formation and the equilibrium constant of complex formation were also obtained by infrared spectral measurement and were used to evaluate free energy and entropy of complex formation. The Badger–Bauer relation was found to exist between $\Delta H°$ and $\Delta\nu_{HF}$. The $\Delta H°$ difference between HF–furan (4.8 kcal mol^{-1}) and HF–2,5-di-MeF (6.74 kcal mol^{-1}) was fairly large, while that between HF–THF (7.36 kcal mol^{-1}) and HF–2,5-di-MeTHF (7.41 kcal mol^{-1}) was almost negligible. Ab initio MO calculations were carried out for HF–furan and HF–THF complexes. The calculated equilibrium geometry and hydrogen bonding energy were in good agreement with the trend of experiments. Component analyses showed that the main difference between the two complexes was in the electrostatic interaction and that the presence of conjugated π electrons changed only the polarization interaction, resulting in a dipole enhancement.

I. Introduction

One of the unique physicochemical properties of hydrogen fluoride (HF) is a strong tendency to form extremely stable hydrogen-bonded complexes with various kinds of organic molecules. The frequency shift ($\Delta\nu_{HF}$) of H–F stretching mode due to hydrogen bond formation and the enthalpies of formation (ΔH) of 1:1 complexes of HF with organic acceptors are found to be larger than the corresponding quantities for any other hydrogen bonding systems.[2] On the other hand, HF has a simple geometric structure and its electronic structure is also relatively simple. These make HF an important substance for theoretical studies on hydrogen bonding.

The thermodynamic data for HF hydrogen-bonded complexes are still limited in number and have so far been obtained from infrared study by using the van't Hoff equation.[3] The best values for the thermodynamic functions of formation reaction of 1:1 complexes may be obtained by combining use of calorimetry with spectroscopic measurement.[4] Therefore, it seems important to establish the calorimetric technique for HF-containing systems. Ab initio SCF molecular orbital (MO) theories have been extensively employed for the prediction of both the geometry and the stabilization energy of many hydrogen-bonded complexes,[5] including those with HF. The energy and charge distribution decomposition (ECDD) analyses of Morokuma[7] and Kitaura–Morokuma[6b] have given theoretical insight into the origin of hydrogen bonding. While experimental results generally reflect only overall properties of the interaction, theoretical studies such as ECDD analysis enable us to understand it more conceptually.

The thermodynamic data to be compared with MO calculations should be those obtained for the complexes in vapor phase. It is impossible to establish such data at the present stage. However, recent infrared studies on the HF–diethyl ether complex indicate that the $\Delta H°$ of this complex in a practically inert solvent (CCl$_4$) coincides with that obtained in vapor phase.[2b,3c] This is further supported by our recent calorimetric study in which we have constructed a new calorimeter and obtained a reliable $\Delta H°$ value for the HF–diethyl ether complex in cyclohexane solution.[8]

In the present study, we attempt to compare the results of theoretical MO calculation with experimental $\Delta H°$ data (obtained in CCl$_4$) for some hydrogen-bonded systems consisting of HF and one of the following four cyclic ethers: furan, tetrahydrofuran (THF), and their derivatives, 2,5-dimethylfuran (2,5-di-MeF) and 2,5-dimethyltetrahydrofuran (2,5-di-MeTHF). The properties of furan and THF as a proton acceptor may be dependent on the difference in the basicity of the acceptor and the presence of conjugated π electrons in the molecule. By studying the hydrogen bonding of HF with these acceptors, one can examine the effects of the difference in such factors and of methyl substitution on the hydrogen bonding.

II. Experimental Section

A. Materials and Preparation of Sample Solution. Hydrogen fluoride and carbon tetrachloride used as an inert solvent were purified in the same manner as described previously.[2b] The dehydration was carefully carried out since the presence of a small amount of water gives rise to H$_2$F$^+$ ion and causes the decomposition of cyclic ethers. The four ethers were obtained from commercial reagents of the highest possible grade and purified by the method recommended in standard texts.[9] These purified liquids were used immediately after the completion of the purification. It should be noted that the commercial reagent of 2,5-di-MeTHF is probably a mixture of cis and trans isomers. It is very difficult to completely separate them from each other.[10] Hence the mixture was simply vacuum distilled twice before use.

The sample solution of HF in CCl$_4$ was prepared in the same manner as described previously,[2b] while the preparation of ether–CCl$_4$ solution was done in the following manner for the purpose of preventing the evaporation of ether. A certain amount (10–20 g) of pure acceptor liquid was first added to pure dehydrated CCl$_4$, which was weighed beforehand in a 100-cm^3 flask, and the flask was reweighed to determine the concentration of ether. The sample solution to be used for the measurements was prepared by transferring 3–5 cm^3 of this standard solution into a weighed flask containing dehydrated CCl$_4$ and then the flask was reweighed.

B. Calorimeter. A new isothermal batch-type calorimeter used in this study has been described elsewhere.[8] The performance of this calorimeter was fully tested by measuring enthalpies of mixing in a binary solution of benzene + chlorobenzene and of the complex formation between HF and diethyl ether in dilute cyclohexane solution.[8] The $\Delta H°$ value was 6.91 ± 0.02 kcal mol^{-1} for the HF–diethyl ether complex. This can be satisfactorily compared with 7.39 ± 0.2 and 7.2 kcal mol^{-1} obtained in CCl$_4$[2b] and vapor phase,[3c] respectively.

C. Infrared Spectral Measurement. The frequency shift $\Delta\nu_{HF}$ of H–F stretching vibration due to complex formation between HF and an acceptor has been determined for the four ethers. The equilibrium

Table I. Equilibrium Constants and Thermodynamic Functions for HF–Ether Hydrogen-Bonded Complexes at 298.15 K

acceptor	K, M^{-1}	$-\Delta G°$, kcal mol^{-1}	$-\Delta H°$, kcal mol^{-1}	$-\Delta S°$, cal mol^{-1} K^{-1}
furan	5.6 ± 1.0	1.0 ± 0.1	4.8 ± 0.2	13 ± 1
2,5-dimethylfuran	59.1 ± 0.5	2.42 ± 0.01	6.74 ± 0.07	14.5 ± 0.3
tetrahydrofuran	1130 ± 80	4.16 ± 0.01	7.36 ± 0.07	10.7 ± 0.3
2,5-dimethyltetrahydrofuran	1440 ± 10	4.31 ± 0.04	7.41 ± 0.12	10.4 ± 0.5
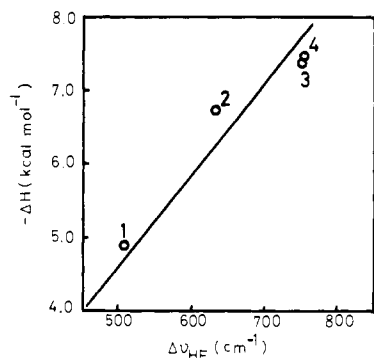
Figure 1. Badger–Bauer plot for HF hydrogen bonding complexes: (1) furan; (2) 2,5-dimethylfuran; (3) tetrahydrofuran; (4) 2,5-dimethyltetrahydrofuran.

constant K of the complex formation has also been evaluated from the analysis of the intensity of associated and free bands. The experimental procedure and apparatus used for obtaining infrared frequency shift and the equilibrium constant have been described previously.[2b]

D. Determination of ΔH. The calorimetric measurements have been done in the following manner. Donor and acceptor solutions are placed separately in two compartments of the calorimeter. By removing the diaphragm between two compartments, both solutions are mixed instantaneously and the heat evolved is detected. Then the enthalpy change ΔH_{obsd} due to hydrogen-bonded complex formation may be given by

$$\Delta H_{obsd} = Q_{obsd} - Q_{dil} (HF) - Q_{dil} (\text{acceptor}) \qquad (1)$$

where Q_{obsd} is the heat evolved when dilute CCl$_4$ solution of HF (proton donor) is mixed with dilute CCl$_4$ solution of proton acceptor, and Q_{dil} (HF) and Q_{dil} (acceptor) are the heats of dilution of HF and acceptor, respectively. Since both Q_{dil} (HF) and Q_{dil} (acceptor) were negligibly small in the concentration range used in the present measurements, ΔH_{obsd} becomes equal to Q_{obsd}. Then the molar enthalpy of hydrogen bond formation ΔH is given by

$$\Delta H = \Delta H_{obsd}/VC_c \qquad (2)$$

where V is the volume of solution and C_c is the molar concentration of the complex which can be calculated by

$$C_c = \frac{(B_t + C_t + 1/K) - [(B_t + C_t + 1/K)^2 - 4B_tC_t]^{1/2}}{2} \qquad (3)$$

where B_t and C_t are total concentrations of acceptor and donor, respectively, and K is the equilibrium constant which is obtained by infrared spectroscopy.[2b] In the present measurements, C_t values determined by the same method as described previously[2b] were between 0.004 and 0.005 M and B_t was 15–20 times as large as C_t, namely, 0.07–0.1 M.

In eq 1 and 2, it is assumed that HF exists as the monomer in the solution before the formation of hydrogen-bonded complex and that only 1:1 hydrogen-bonded complex is formed when HF solution is mixed with proton acceptor solution. Both postulates are proved to be fulfilled in the present measurements.[8]

The accuracy of ΔH values greatly depends on the C_c value. This means that K should be determined very accurately. Fortunately, for complexes with strong bases such as THF and 2,5-di-MeTHF which have a large K value, C_c is almost equal to C_t in eq 2 when $B_t \gg C_t$. Hence C_c is almost unchanged even if the K value is somewhat altered. On the other hand, in the case of complexes with weak bases such as furan for which the K value is fairly small, an approximate relation,

Table II. Spectral Properties of HF–Ether Complexes

donor	acceptor	ν_{HF},[a] cm^{-1}	$\Delta\nu_{HF}$, cm^{-1}
HF	in vapor phase[b]	3961[c]	0
	in CCl$_4$	3856	105
	furan	3454	507
	2,5-dimethylfuran	3330	631
	tetrahydrofuran	3210	751
	2,5-dimethyltetrahydrofuran	3202	759

[a] Data obtained at 25 °C. [b] H. Hyman and J. J. Katz, "Non-Aqueous Solvent System", T. C. Waddington, Ed., Academic Press, New York, N.Y., 1965. [c] This is due to the absorption of HF monomer and may be used as the reference for $\Delta\nu_{HF}$.

$C_c \approx C_t$, cannot be assumed even if $B_t \gg C_t$ and the error in K results in the decrease in the precision of ΔH (see Table I).

E. Thermodynamic Functions of Hydrogen-Bonded Complexes: Experimental Results. From the results of the above-mentioned calorimetric and spectral measurements, the equilibrium constant K and thermodynamic functions, $\Delta G°$, $\Delta H°$, and $\Delta S°$ for the formation of hydorgen-bonded complexes were evaluated for four HF–ether systems with high precision. The results are summarized in Table I. The present $\Delta G°$ and $\Delta H°$ values are larger than those for other hydrogen-bonding systems.[4a] Even in phenol hydrogen-bonding systems which have relatively large $\Delta H°$ values, the phenol–THF complex has a $\Delta H°$ value of 5.19 kcal mol^{-1},[11] which is to be compared with the present value for HF–THF, 7.36 kcal mol^{-1}. On the other hand, $\Delta S°$ values for HF hydrogen-bonded complexes which are in the range between -10 and -15 cal K^{-1} mol^{-1} are almost comparable with those for other hydrogen-bonding systems.[4a]

As expected from the difference in the basicity of the acceptors,[12] a distinct difference in $\Delta H°$ can be observed between HF–furan and HF–THF complexes. Furthermore, there exists between both complexes an apparent difference in the methyl-substituent effect, which will be discussed in section IV.

In the case of HF-2,5-di-MeTHF complex, the results obtained are those for a mixture of cis and trans isomers. However, the present $\Delta H°$ value may be regarded as correct for both isomers because the difference between their basicities[12] is almost negligible and only a single hydrogen-bonded band of ν_{HF} can be detected in the spectrum of the HF-2,5-di-MeTHF system.

The infrared spectral data for HF–ether complexes are given in Table II. As shown in Figure 1, a linear correlation which is known as the Badger–Bauer relationship can be recognized between $\Delta H°$ and $\Delta\nu_{HF}$. The slope of the linear correlation is comparable with that obtained previously.[2b]

F. Electronic Contribution to ΔH. The ΔH value obtained from calorimetry consists of several contributions

$$\Delta H = \Delta E(\text{electronic}) + \Delta E(\text{trans}) + \Delta E(\text{rot})$$
$$+ \Delta E(\text{vib}) + \Delta(PV) \qquad (4)$$

where $\Delta E(\text{trans})$, $\Delta E(\text{rot})$ and $\Delta E(\text{vib})$ are respectively the change in translational, rotational, and vibrational energies due to the formation of the hydrogen-bonded complex. Since only the electronic energy can be obtained by MO calculations, other terms must be evaluated with conventional methods[4a] and subtracted from ΔH to obtain $\Delta E(\text{electronic})$.

The translational and rotational energies in HF hydrogen-bonding systems can be given by

$$\Delta E(\text{trans}) + \Delta E(\text{rot}) = -(5/2)RT \qquad (5)$$

When a hydrogen bond is formed, fundamental frequencies of the proton acceptor remain almost unchanged, and it will be sufficient

Table III. Calculation of Total Electronic Energy Change Contribution to Experimental Enthalpy Value (kcal mol⁻¹) at 298.15 K

	HF–(CH)₄O	HF–(CH₂)₄O
$\Delta H°$ (experimental)	−4.8 ± 0.2	−7.36 ± 0.07
$-\Delta E°$ (translational)	+0.889($3RT/2$)	+0.889($3RT/2$)
$-\Delta E°$ (rotational)	+0.593(RT)	+0.593(RT)
$-\Delta E°$ (complex vibration-corresponding HF monomer vibration)[a]	+0.725	+1.074
$-\Delta E°$ (5 weak complex vibrations)[b]	−2.963($5RT$)	−2.963($5RT$)
$-\Delta(PV)$	+0.593(RT)	+0.593(RT)
$\Delta E°$ (electronic)	−5.0 ± 0.2	−7.17 ± 0.07

[a] When hydrogen-bonded complexes are formed, the main change of vibrations in each molecule is assumed to be that in the H–F stretching vibration, and hence the contributions of other changes in fundamental frequencies of acceptor monomer can be neglected. [b] These new vibrations with hydrogen bonding could not be identified. The classical limit, RT, was used for each weak complex mode.

to take account of only the changes in fundamental frequencies of the proton donor. In the case of HF, only the contribution from the change in H–F stretching vibration frequency needs to be considered. The vibrational energy can then be calculated by

$$h\nu\{(^1/_2) + [\exp(h\nu/RT) - 1]^{-1}\} \qquad (6)$$

Another contribution is due to vibrations corresponding to the motion of one monomer unit relative to the other. Since they are expected to occur at low frequencies, the classical energy RT may be used as an average value for each vibration. The contributions of these factors to the $\Delta H°$ for both HF–furan and HF–THF complexes are summarized in Table III.

One can see from these results that, in both complexes studied, the sum of $\Delta E°$(trans), $\Delta E°$(rot), $\Delta E°$(vib), and $\Delta(PV)$ is fairly small because of cancellation between them. Then $\Delta E°$(electronic) should become almost equal to $\Delta H°$, except for a minor correction due to solvation energy in CCl₄. However, this effect will be small since there is no significant difference between the $\Delta H°$ value for HF–diethyl ether obtained in the vapor phase[3c] and that in CCl₄ solution.[2b]

III. Theoretical Section

The energy decomposition analysis of Kitaura–Morokuma[6b] within the ab initio SCF theory is performed for both HF–furan and HF–THF complexes.

A. Method of Calculation. All the calculations of hydrogen bond energy ΔE have been carried out within the closed shell LCAO–SCF–MO approximation. The GAUSSIAN 70 program with Morokuma's ECDD analysis routines has been used.[13]

The STO-3G basis set[14] was used to obtain the optimum geometries of complexes and the 4-31G basis set[15] was used in other calculations. Neither the STO-3G nor 4-31G basis set is adequate for quantitative accuracy, but it has been reported that the latter could give a more reliable description of hydrogen bonding.[5,16]

The ECDD analysis has been performed with the method of Kitaura and Morokuma.[6b] A full account of this method has been given elsewhere.[6] In this method, the total interaction energy ($\Delta E = E_{\text{complex}} - E_{\text{monomers}}$) and the charge distribution rearrangement ($\Delta\rho(r) = \rho(r)_{\text{complex}} - \rho(r)_{\text{monomers}}$) can be decomposed in the following manner:

$$\Delta E = \text{ES} + \text{PL} + \text{EX} + \text{CT} + \text{MIX} \qquad (7)$$

$$\Delta\rho(r) = \rho_{\text{PL}}(r) + \rho_{\text{EX}}(r) + \rho_{\text{CT}}(r) + \rho_{\text{MIX}}(r) \qquad (8)$$

ES is the electrostatic interaction between the undistorted electron distribution of a monomer A and that of a monomer B. PL is the polarization interaction, namely, the effect of distortion of the electron distribution of A by B (and vice
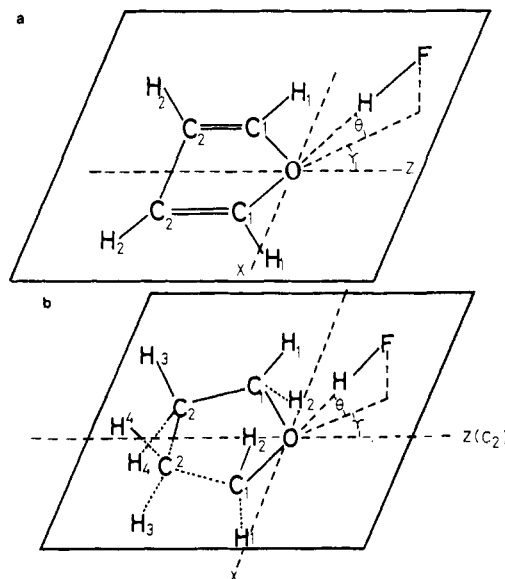
Figure 2. (a) Geometry of HF–furan system. (b) Geometry of HF–tetrahydrofuran system.

versa). EX is the exchange repulsion interaction caused by the exchange of electrons between A and B. CT is the charge transfer or electron delocalization interaction caused by the transfer of charge from occupied MOs of A to vacant MOs of B (and vice versa). MIX is the coupling interaction, which is calculated as the difference between the total SCF interaction energy ΔE and the sum of the above four components.

B. Geometries. The geometry of furan was taken from experiments.[17] In Figure 2a, $R(C_2C_2) = 1.4309$ Å, $R(C_1C_2) = 1.3609$ Å, $R(C_1O) = 1.3621$ Å, $R(C_1H_1) = 1.0750$ Å, $R(C_2H_2) = 1.0768$ Å, $\angle C_1C_2C_2 = 106.05°$, $\angle C_2C_1O = 110.68°$, $\angle C_1OC_1 = 106.55°$, $\angle OC_1H_1 = 115.92°$, and $\angle C_2C_2H_2 = 127.95°$. The geometry of THF adopted was the most stable form estimated by an ab initio calculation using the 6-31G basis set.[18] As shown in Figure 2b, it has a twist or half-chair conformation which belongs to the point group C_2. The standard values of Pople and Gordon[19] were used for the lengths and angles: $R(C_1O) = 1.43$ Å, $R(C_1C_2) = R(C_2C_2) = 1.54$ Å, $R(C_1H_1) = R(C_2H_2) = 1.09$ Å, $\angle C_1OC_1 = 111.60°$, $\angle OC_1C_2 = 105.56°$, $\angle C_1C_2C_2 = 107.95°$, $\angle OC_1H_1 = \angle OC_1H_2 = \angle C_2C_1H_1 = \angle C_2C_1H_2 = 110.44°$, and $\angle C_1C_2H_3 = \angle C_1C_2H_4 = \angle C_2C_2H_3 = \angle C_2C_2H_4 = 111.33°$.

For the HF monomer, the optimized STO-3G bond distance[20] ($R(\text{HF}) = 0.956$ Å) was used in STO-3G calculations, while the experimental value[21] ($R(\text{HF}) = 0.9171$ Å) was employed in 4-31G calculations so as to compare with other published results. The monomer geometries were held rigid for all the calculations. The hydrogen bond was assumed to be linear; namely, HF and the oxygen atom are collinear. For the HF–furan system, the z axis is the C_2 symmetry axis and the xz plane is the molecular plane of furan. For HF–THF, the z axis is the C_2 symmetry axis and the xz plane is the plane defined by the O atom and the two C_1 atoms. The angle θ between the intermolecular axis and the xz plane is first optimized by keeping the F–O distance $R(\text{F–O})$ constant. Next, $R(\text{F–O})$ is optimized by keeping θ at its optimum value. The angle γ is assumed to be zero.

It has been reported that the optimum intermolecular distance estimated with the STO-3G set is shorter than that with the 4-31G set.[22] Hence, in 4-31G calculations, we use the value of STO-3G optimum intermolecular distance, $R_{\text{op}}(\text{F–O})$, scaled by utilizing the results for the HF–H₂O complex; it is multiplied by 1.015, the ratio of the optimum intermolecular distance for HF–H₂O, R_{op} (4-31G)/R_{op} (STO-3G).[23,24]

Table IV. Optimum Geometry, Hydrogen Bond Energy, and Energy Components (kcal mol^{-1}) for HF–Furan and HF–Tetrahydrofuran

	HF–(CH)$_4$O		HF–(CH$_2$)$_4$O	
basis set	STO-3G	4-31G	STO-3G	4-31G
optimum geometry				
R(F–O), Å	2.785	2.828[a]	2.644	2.685[a]
θ	0.0	0.0	0.0	0.0
hydrogen bond energy				
ΔE	−3.63	−8.95	−7.35	−14.40
ΔE_{scaled}		−5.26		−9.89
ΔE_{obsd}		−5.0 ± 0.2		−7.17 ± 0.07
components				
ES$_{scaled}$		−6.43		−12.83
ES		−10.12		−17.34
EX		4.48		8.39
CT		−1.95		−3.06
CT(B → A)[b]		−1.70		−2.69
CT(A → B)[b]		−0.24		−0.37
PL		−1.15		−1.88
PL(A)[c]		−0.15		−0.41
PL(B)[c]		−0.92		−1.31
MIX		−0.21		−0.51

[a] Estimated from the results of STO-3G. [b] CT(B → A) is the contribution of the charge transfer from proton acceptor to proton donor and CT(A → B) is the contribution of the charge transfer from proton donor to proton acceptor. [c] PL(A) is the polarization of proton donor and PL(B) is the polarization of proton acceptor.
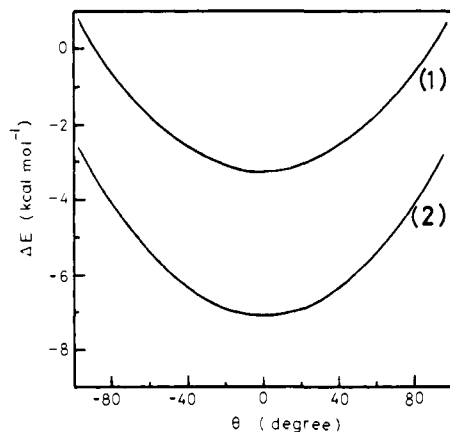

Figure 3. Hydrogen bond energy as a function of θ: (1) HF–furan, R(F–O) = 3.0 Å; (2) HF–tetrahydrofuran, R(F–O) = 2.8 Å.

C. Computational Results. (1) Geometry and Potential Curves.

The optimized values of θ and R(F–O) with the STO-3G set both for HF–furan and HF–THF complexes are given in Table IV. The optimized θ values are zero for both complexes; HF is on the molecular axis of the proton acceptor. One might have expected $\theta \sim 55°$ if hydrogen bonding is assumed to take place in the direction of the sp^3-hybridized lone pair of the oxygen atom. The potential curves obtained as functions of θ are shown in Figure 3. The potential curves as functions of R(F–O) are shown in Figure 4. As expected, the stronger complex has a smaller R_{op}(F–O). The values of second derivatives of the hydrogen bond energy with respect to R(F–O) and θ are given in Table V. One finds that the force constant with respect to R(F–O) depends on the hydrogen bond strength, while the one with respect to θ does not.

The optimum value of θ could depend on the basis set. In the case of HF–H$_2$O, for example, the STO-3G calculation gives $\theta = 35°$,[23] while $\theta = 0$ in the 4-31G calculation.[24] A 4-31G calculation gave $\theta = 0$ for the HF–dimethyl ether complex,[24] in which the oxygen atom is in an environment similar to that of the present complexes. As shown in Table VI, 4-31G calculations, as well as STO-3G calculations, for HF–furan actually give $\theta = 0$.

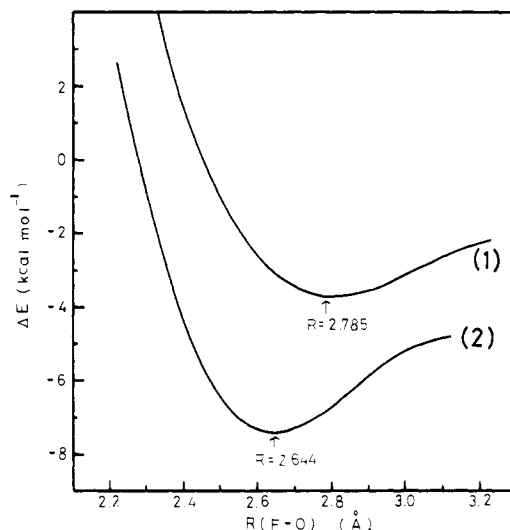Now we ask which factor determines θ. In the case of small

Figure 4. Hydrogen bond energy as a function of R(F–O) at $\theta = 0$: (1) HF–furan; (2) HF–tetrahydrofuran.

Table V. Values of Second Derivatives of Intermolecular Energies[a]

	HF–(CH)$_4$O	HF–(CH$_2$)$_4$O
$\partial^2 E / \partial X^2$		
$X = R$(F–O)	30.16 (0.2095[b])	65.85 (0.4575[b])
$X = \theta$	8.31 × 10^{-4}	9.35 × 10^{-4}

[a] The STO-3G basis set was used. E, R, and θ are expressed in kcal mol^{-1}, Å, and deg, respectively. [b] In mdyn Å^{-1}.

complexes such as (H$_2$O)$_2$, (HF)$_2$, and HF–NH$_3$, the factor determining θ has been studied in detail by the energy decomposition analysis.[5] In a large complex there are atoms which do not directly participate in hydrogen bonding, but give rise to additional local polarities. It is interesting to examine effects of these polarities on θ in HF–furan as compared with HF–H$_2$O. As θ increases, HF should be influenced by the local polarities of the C$_1$–H$_1$ and C$_2$–H$_2$ bonds as well as π electrons.

Given in Table VI are the energy components as functions of θ for both HF–H$_2$O and HF–furan at their equilibrium

Table VI. Energy Components (kcal mol^{-1}) for HF–H$_2$O and HF–(CH)$_4$O as Functions of θ Using 4-31G Basis Set

| | | HF–H$_2$O R(F–O) = 2.64 Å^a | | | HF–(CH)$_4$O R(F–O) = 2.828 Å^b | | | HF–H$_2$O R(F–O) = 2.828 Å^c | |
	0.0°	54.73°	90.0°	0.0°	54.73°	90.0°	0.0°	54.73°	90.0°
θ									
ΔE	−13.42	−11.79	−7.09	−8.95	−6.94	−3.29	−12.46	−11.21	−7.56
ES	−18.22	−17.01	−12.15	−10.12	−8.25	−5.04	−13.52	−12.21	−8.18
EX	9.53	10.60	11.22	4.48	4.79	5.99	4.34	4.87	5.17
CT	−2.90	−3.59	−4.40	−1.95	−2.21	−2.69	−2.11	−2.79	−3.61
PL	−1.48	−1.14	−0.92	−1.15	−1.01	−1.11	−0.95	−0.71	−0.50
MIX	−0.35	−0.65	−0.84	−0.21	−0.26	−0.44	−0.22	−0.37	−0.44

^{a} This value was optimized by Kollman and Rothenberg (ref 24) with the 4-31G basis set. ^{b} The equilibrium intermolecular distance. ^{c} This value is the same as that of the equilibrium intermolecular distance for HF–(CH)$_4$O.

distance, as well as for HF–H$_2$O at R_{op}(F–O) of HF–furan. One can see for each complex that ES decreases drastically with increasing θ and is the main controlling factor in determining θ. Additional local polarities in furan do not affect the angular dependence of ES. Apparently even for a large acceptor molecule, θ is controlled by the local interaction in the hydrogen-bonding region.

A difference between the two complexes can be recognized in the change of PL with θ. Its absolute value decreases monotonically with θ for HF–H$_2$O, while it is almost unchanged for HF–furan. This difference can be attributed to the fact that furan has a conjugated π-electron system which is easily polarized, particularly when an HF molecule approaches from the direction of $\theta = 90°$.

(2) Decomposition Analysis of Energy at the Equilibrium Geometry. The energy decomposition analysis for both HF–furan and HF–THF complexes has been carried out with the 4-31G basis set. The results are summarized in the lower half of Table IV. Since ES is overestimated in the 4-31G calculation, it is scaled in the same manner as described by Umeyama and Morokuma.^{5} The scaling is done by multiplying by the ratio

$$\left[\frac{\mu(\text{acceptor, obsd}) \, \mu(\text{HF, obsd})}{\mu(\text{acceptor, 4-31G}) \, \mu(\text{HF, 4-31G})} \right]^{1/2} \quad (9)$$

Scaled values of ES(ES$_{scaled}$) and ΔE obtained by using ES$_{scaled}$ (ΔE_{scaled}) at equilibrium geometry are also given in Table IV.

We first compare ΔE_{scaled} with ΔE_{obsd} in Table IV. The calculated results well represent the trend of experimental data. Absolute values of the electronic energy can also be compared satisfactorily with the experiment.

Next we examine the results of decomposition of the electronic energy ΔE_{scaled}. Qualitatively, both complexes are principally ES in nature, with a nonnegligible contribution of CT—the same trend as has been observed on most of the hydrogen-bonded complexes.^{5} The total interaction energy consists of 66 (75) % ES, 20 (15) % CT, 12 (9) % PL, and 2 (2)% MIX for HF–furan and of 70 (76)% ES, 16 (13)% CT, 10 (8)% PL, and 3 (2)% MIX for HF–THF (the numbers in parentheses are for the unscaled energy); these results can be compared with 75 (79)% ES, 16 (13)% CT, 8 (6)% PL, and 2 (2)% MIX for HF–H$_2$O.

The results of detailed analyses for both CT and PL are also included in Table IV. As for the CT stabilization, further division of CT indicates that most of the CT energy is due to the charge transfer from proton acceptor to proton donor (CT(B → A)). On the other hand, the results of the decomposition of PL indicate for each complex that the major contribution to total PL comes from PL of the acceptor PL(B).

In order to examine slight differences among the three complexes in more detail, a comparison has been made with the results of an energy decomposition at a fixed R(F–O), 2.685 Å, which is the same as that in the equilibrium geometry

Table VII. Comparison of Energy Components (kcal mol^{-1}) for Three Complexes at a Fixed R(F–O)^a

	HF–H$_2$O	HF–(CH)$_4$O	HF–(CH$_2$)$_4$O
ΔE_{scaled}	−9.13	−4.57	−9.89
ΔE	−13.30	−9.31	−14.40
ES$_{scaled}$	−12.74	−8.27	−12.83
ES	−16.91	−13.01	−17.34
EX	7.90	8.16	8.39
CT	−2.65	−2.54	−3.06
PL	−1.33	−1.67	−1.88
PL(A)^b	−0.40	−0.18	−0.41
PL(B)^b	−0.83	−1.37	−1.31
MIX	−0.33	−0.25	−0.51

^{a} R(F–O) is the same value as that of HF–(CH$_2$)$_4$O, 2.685 Å. ^{b} PL(A) and PL(B) are the polarization of HF and proton acceptor, respectively.

Table VIII. Further Decomposition of CT and PL Energies (kcal mol^{-1}) for HF–(CH)$_4$O System at R(F–O) = 2.828 Å Using the 4-31G Basis Set^a

CT	(CH)$_4$O → HF	HF → (CH)$_4$O	total
σ	−1.70	−0.22	−1.92
π	−0.01	−0.02	−0.03
total	−1.71	−0.24	−1.95

PL	(CH)$_4$O	HF	total
σ	−0.76	−0.15	−0.91
π	−0.26	0.00	−0.26
total	−1.02	−0.15	−1.17

^{a} Couplings between individual terms are small and are not listed.

for HF–THF. The results are summarized in Table VII. It is found that ES (or ES$_{scaled}$) decreases in the order HF–THF > HF–H$_2$O > HF–furan. The difference in ES between HF–THF (or HF–H$_2$O) and HF–furan is particularly large, as reflected in the difference in hydrogen bond energy. No significant differences can be recognized among EX values for three complexes at an identical intermolecular distance. This indicates that EX does not depend on the inherent property of proton acceptors, but rather on the intermolecular distance. CT also increases in the order of the hydrogen bond strength: HF–furan < HF–H$_2$O < HF–THF. Finally PL increases in the order HF–H$_2$O < HF–furan < HF–THF, which is parallel with the size of proton acceptor molecule. It is also interesting that PL(B) for HF–furan is greater than that for HF–THF. This is presumably due to the fact that there exist conjugated, easily polarizable π electrons in furan.

Further analyses have been carried out for CT and PL of HF–furan in order to examine the function of π electrons in detail. The results are given in Table VIII. The major portion of CT stabilization is due to furan → HF transfer via σ orbitals,

Table IX. Decomposition Analysis of Mulliken Gross Population Change in HF–Furan System Using the 4-31G Basis Set[a]

	F	H	O	C_1	C_2	H_1	H_2	$\Delta Q(A \leftarrow B)$[b]
ρ[c]	9.4786	0.5214	8.6772	5.8448	6.2602	0.7705	0.7859	
$\Delta\rho$	73	−49	85	−18	−7	−16	−13	24
π	0		29	4	−18			
σ	73		56	−21	11			
ρ_{EX}	9	−9	−1	0	0	0	0	
π	0		0	0	0			
σ	9		−1	0	0			
ρ_{CT}	−4	25	−20	0	−1	0	0	22
π	0		0	0	0			
σ	−3		−21	0	−1			
ρ_{PL}	31	−31	92	−11	−9	−15	−12	
π	0		26	3	−16			
σ	31		66	−14	7			
$\rho_{PL}(A)$[d]	21	−21						
$\rho_{PL}(B)$[d]			88	−10	−8	−14	−11	
ρ_{MIX}	36	−34	13	−8	2	−2	−1	2
π	0		3	1	−2			
σ	36		10	−8	4			

[a] Obtained at $R(F-O) = 2.685$ Å (the equilibrium geometry for HF–THF). Changes in population are in the unit of 10^{-3}. [b] Net charge transfer from furan to HF. [c] Gross atomic population of monomer. [d] $\rho_{PL}(A)$ and $\rho_{PL}(B)$ are the polarization of HF and furan, respectively.

Table X. Decomposition Analysis of Mulliken Gross Population Change in HF–Tetrahydrofuran System Using the 4-31G Basis Set[a]

	F	H	O	C_1	C_2	H_1	H_2	H_3	H_4	$\Delta Q(A \leftarrow B)$[b]
ρ[c]	9.4786	0.5214	8.7213	5.9463	6.3650	0.8293	0.8404	0.8272	0.8310	
$\Delta\rho$	84	−50	68	−2	−1	−15	−16	−8	−10	35
π	0		12	14	6					
σ	85		56	−16	−7					
ρ_{EX}	10	−10	−1	1	0	0	0	0	0	
π	0		0	0	0					
σ	10		−1	1	0					
ρ_{CT}	−4	32	−26	0	−1	0	0	0	−1	29
π	0		0	0	0					
σ	−4		−27	0	−1					
ρ_{PL}	44	−44	93	−2	−2	−13	−14	−7	−9	
π	0		11	11	5					
σ	44		82	−14	−7					
$\rho_{PL}(A)$[d]	36	−36								
$\rho_{PL}(B)$[d]			87	−2	−2	−12	−13	−6	−8	6
ρ_{MIX}	34	−28	3	0	2	−2	−3	−1	−1	
π	0		1	2	1					
σ	34		2	−2	1					

[a] Obtained at $R(F-O) = 2.685$ Å (the equilibrium geometry). Changes in population are in the unit of 10^{-3}. [b] Net charge transfer from THF to HF. [c] Gross atomic population of monomer. [d] $\rho_{PL}(A)$ and $\rho_{PL}(B)$ are the polarization of HF and THF, respectively.

namely, the charge transfer from occupied σ orbitals of furan to vacant σ orbitals of HF, and the remaining portion is mostly due to the HF → furan σ back-donation. Contributions of π orbitals to CT are shown to be negligibly small. The major portion of PL stabilization is due to the polarization of furan σ orbitals. However, a considerable contribution of furan π orbitals is also recognized.

(3) Atomic Population Change Due to Hydrogen Bond Formation. Changes in gross atomic population due to hydrogen bond formation have been calculated for both complexes using the 4-31G set. The results are shown in Tables IX and X. In accordance with the previously observed general trend,[25] EX removes a small amount of electron cloud from the interaction region and depends on the intermolecular distance, as was shown for the energy. CT causes local charge redistributions on the oxygen atom of the proton acceptor and on the hydrogen-bonding proton. As was seen for ΔE, π orbitals do not participate in the charge transfer and most part of CT consists of the charge transfer from the proton acceptor to the proton donor via σ orbitals. The total amount of charge transferred depends on the strength of the hydrogen bond.

The electron redistribution due to PL is large and is exerted on all the atoms. Its effect on the proton acceptor is to accumulate electrons on the interaction side. One can see that both σ and π orbitals contribute to PL, as was the case for ΔE. The influence of the conjugated π electrons in furan can be clearly observed in comparison with the results for HF–THF. The change in the electron population on the oxygen atom of HF–furan is greater than that of HF–THF because of the increase in π-electron density due to PL.

From the above analysis, one may conclude that charge redistribution due to the hydrogen bond formation is caused mainly by PL, with minor contributions of CT and MIX. Similar results have been reported previously.[5,25]

The changes in the H–F overlap population due to hydrogen bond formation have been calculated by using the 4-31G basis set. The results are given in Table XI. The overlap population on the H–F bond decreases for both complexes. The decrease will weaken the H–F bond and leads to a decrease in the force constant of the bond, namely, a hydrogen bond shift of the H–F stretching vibration. As is expected, the trend of the population decrease coincides with that of the frequency shift (see Table

Table XI. Decomposition Analysis of Mulliken Population Change on H–F Bond at the Equilibrium R(F–O) with the 4-31G Basis Set

	HF–(CH)$_4$O	HF–(CH$_2$)$_4$O
HF monomer	0.2105	0.2105
complex	0.2063	0.2033
total change[a]	−42	−72
EX	12	24
CT	−35	−46
CT(B → A)[b]	−31	−46
CT(A → B)[b]	−3	2
PL	−2	−10
PL(A)[c]	−6	−13
MIX	−17	−40

[a] Change in population is in unit of 10^{-4}. [b] CT(B → A) is the charge transfer from proton acceptor to HF and CT(A → B) is the charge transfer from HF to proton acceptor. [c] PL(A) is the polarization of HF.

II). The decomposition analysis indicates that EX causes the increase of electrons in the range of H–F bond, while CT causes a large decrease.

(4) Decomposition Analysis for Dipole Moment Enhancement. The enhancement of the dipole moment is one of the most recognizable features of the hydrogen bonding. Calculated values of the dipole moment are given in Table XII. The dipole moment enhancement $\Delta\mu$ can be attributed mainly to PL supplemented by CT and MIX. This is expected from the largest contribution of PL in the electron redistribution. It should be noted that the PL component of the proton acceptor, μ_{PL}(B), for HF–furan is almost as large as that for HF–THF, a stronger complex.

IV. Discussion and Conclusion

A. Role of Conjugated π-Orbitals in Proton Acceptor: Comparison between Furan and Tetrahydrofuran. Though both HF–furan and HF–THF complexes have an oxygen atom of the same ether link as the proton acceptor, we observed in the present experiment substantial differences both in ΔH° and $\Delta\nu_{HF}$. The present MO calculation can well describe the trend of the experiment. The ECDD analysis has furnished useful information concerning the source of differences between furan and THF as proton acceptor. The difference lies in the fact that furan has conjugated π electrons, while THF does not. Electrons on the oxygen atom in furan delocalize through conjugated π orbitals to decrease the net charges on the oxygen atom and lower the ability as the proton acceptor, as compared with that in THF. Actually the difference in hydrogen bond energy between the two complexes is principally due to ES. π orbitals do not play a primary role in CT. A distinct difference due to conjugated π electrons can be seen in the polarization of the proton acceptor. For example, a comparison at the same F–O distance has indicated that the PL(B) energy for HF–furan is larger than that for the HF–THF complex. A much larger effect of π electrons can be seen in the effect of PL on the electron redistribution; the change in electron population on the oxygen atom of HF–furan is greater than that of HF–THF because of PL effect. The trend of the dipole moment enhancement is also consistent with that of the electron redistribution.

However, the contributions of each component to the total attractive energy were found to be similar for both complexes, the effect of conjugated π-electron systems being minor. We therefore conjecture that the success of the present Badger–Bauer correlation given in Figure 1 has to do with this similarity in the contributions of each component, especially of the ES component, which is essentially the critical factor in the hydrogen bonding interaction.

Table XII. Decomposition Analysis for the Enhancement of Dipole Moment (D) with the 4-31G Basis Set[a]

	HF–(CH)$_4$O	HF–(CH$_2$)$_4$O
HF monomer	2.281 (1.8195)[b]	
acceptor monomer	1.306 (0.661)[c]	2.476 (1.70)[c]
monomer vector sum	3.587	4.757
complex	4.524	5.819
$\Delta\mu$	0.937	1.062
μ_{EX}	0.019	0.030
μ_{CT}	0.128	0.176
μ_{CT}(B → A)	0.140	0.172
μ_{CT}(A → B)	−0.011	0.007
μ_{PL}	0.698	0.785
μ_{PL}(A)	0.090	0.159
μ_{PL}(B)	0.544	0.558
μ_{MIX}	0.092	0.071

[a] A is HF and B is proton acceptor. [b] Experimental value: R. Weiss, *Phys. Rev.*, **131**, 659 (1963). [c] Experimental value. Reference 17.

Table XIII. STO-3G Gross Atomic Populations of Acceptor Monomers and Dipole Moments[a]

	furan	2,5-dimethyl-furan	tetrahydro-furan	2,5-dimethyl-tetrahydro-furan[b]
dipole moment, D	0.43	0.005	1.601	1.484
atomic population on oxygen	8.2002	8.2139	8.2670	8.2764

[a] The substituted molecules have the same geometry as that of the corresponding unsubstituted molecule. [b] The trans isomer was calculated.

B. Substituent Effect. The present calorimetric and spectroscopic measurements have revealed that the ΔH° for HF–2,5-di-MeF is much larger than that for HF–furan, while the ΔH° for HF–2,5-di-MeTHF is almost as large as that for HF–THF, and that the $\Delta\nu_{HF}$ values are consistent with the trend of ΔH°. It is therefore interesting to consider the origin of this difference in the substituent effect to ΔH°.

For this purpose, MOs of substituted proton acceptors were calculated with the STO-3G basis set and some results are shown in Table XIII. The gross atomic population on the oxygen atom is larger in the substituted acceptor than in the corresponding nonsubstituted monomer. This local increase in the electron population on the oxygen atom should lead to an increase in the attractive contributions of ES and CT, except for possible minor contributions of local polarities of the substituent groups. The PL component should also increase by substitution because the polarization would increase with the size of the molecule.[5] Judging from Table XIII, however, it is unlikely that the substituent effects to ES, CT, and PL differ substantially between furan and THF.

Therefore we conjecture that the difference in the ΔH substituent effect is probably due to that in EX. The equilibrium intermolecular distance in HF–THF is expected to be shorter (~0.14 Å by our estimate) than that in the HF–furan complex. The EX repulsion increases more rapidly than the attractive components as the distance decreases. Our conjecture is that for HF–2,5-di-MeTHF a large increase in EX repulsion completely cancels out with the increase in the attractions, resulting in no substituent effect in ΔH. For HF–2,5-di-MeF, which is more loosely complexed, there will remain a net increase in the attraction, hence a substituent effect. This conjecture was not tested in the present paper.

We finally mention the local nature of the electrostatic interaction. The dipole moment of 2,5-di-MeF or 2,5-di-MeTHF is calculated to be much smaller than that of the corresponding nonsubstituted ether (see Table XIII). If the predominant factor in ES is of the point dipole–dipole type, the hydrogen bond energy as well as ES should decrease in the substituted complexes. However, the fact that the observed $\Delta H°$ for the HF-2,5-di-MeF complex is much larger than that for the HF-furan complex suggests that the critical factor in determining ES is not the overall molecular polarity as expressed by the dipole moment, but rather the local polarities in the hydrogen-bonding region.[5]

References and Notes

(1) (a) Kyoto University; (b) Institute for Molecular Science.
(2) (a) H. Touhara, H. Shimoda, K. Nakanishi, and N. Watanabe, *J. Phys. Chem.*, **75**, 2222 (1971); (b) M. Tsuda, H. Touhara, K. Nakanishi, and N. Watanabe, *ibid.*, **80**, 362 (1976); (c) *Bull. Chem. Soc. Jpn.*, **49**, 2391 (1976).
(3) (a) D. N. Schepkin, *Opt. Spectrosk.*, **19**, 709 (1965); (b) D. N. Schepkin, *Teor. Eksp. Khim.*, **2**, 276 (1966); (c) R. K. Thomas, *Proc. R. Soc. London, Ser. A*, **322**, 137 (1971).
(4) (a) M. D. Joesten and L. J. Schaad, "Hydrogen Bonding", Marcel Dekker, New York, N.Y., 1974; (b) D. V. Fenby and L. G. Hepler, *Chem. Soc. Rev.*, **3**, 193 (1974).
(5) H. Umeyama and K. Morokuma, *J. Am. Chem. Soc.*, **99**, 1316 (1977), and references cited therein.
(6) (a) K. Morokuma, *J. Chem. Phys.*, **55**, 1236 (1971); (b) K. Kitaura and K. Morokuma, *Int. J. Quantum Chem.*, **10**, 325 (1976).
(7) K. Morokuma, *Acc. Chem. Res.*, **10**, 294 (1977).
(8) M. Tsuda, H. Touhara, K. Nakanishi, and N. Watanabe, *Netsusokutei*, **5**, 57 (1978).
(9) J. A. Riddick and W. B. Bunger, "Organic Solvents", 3rd ed., Wiley-Interscience, New York, N.Y., 1970.
(10) D. J. Goldsmith, E. Kennedy, and R. G. Campbell, *J. Org. Chem.*, **40**, 3571 (1975).
(11) R. West, D. L. Powell, M. K. T. Lee, and L. S. Whatley, *J. Am. Chem. Soc.*, **86**, 3227 (1964).
(12) E. M. Arnett, *Prog. Phys. Org. Chem.*, **1**, 233 (1963).
(13) The IMS version of W. J. Hehre, W. A. Lathan, R. Ditchfield, M. D. Newton, and J. A. Pople, "GAUSSIAN 70", Program No. 236, Quantum Chemistry Program Exchange, Indiana University.
(14) W. J. Hehre, R. F. Stewart, and J. A. Pople, *J. Chem. Phys.*, **51**, 2657 (1969).
(15) R. Ditchfield, W. J. Hehre, and J. A. Pople, *J. Chem. Phys.*, **54**, 724 (1971).
(16) (a) A. Johansson, P. Kollman, and S. Rothenberg, *Theor. Chim. Acta*, **29**, 167 (1973); (b) A. Johansson, P. Kollman, S. Rothenberg, and J. McKelvey, *J. Am. Chem. Soc.*, **96**, 3794 (1974).
(17) Nihon-kagaku-kai, Ed., "Kagaku-binran", 2nd ed., Maruzen, Tokyo, 1975, p 1398.
(18) D. Cremer and J. A. Pople, *J. Am. Chem. Soc.*, **97**, 1358 (1975).
(19) J. A. Pople and M. S. Gordon, *J. Am. Chem. Soc.*, **89**, 4253 (1967).
(20) M. D. Newton, W. A. Lathan, W. J. Hehre, and J. A. Pople, *J. Chem. Phys.*, **52**, 4064 (1970).
(21) G. Herzberg, "Spectra of Diatomic Molecules", Van Nostrand, Princeton, N.J., 1950.
(22) W. C. Topp and L. C. Allen, *J. Am. Chem. Soc.*, **96**, 5291 (1974).
(23) P. Kollman, A. Johansson, and S. Rothenberg, *Chem. Phys. Lett.*, **24**, 199 (1974).
(24) P. Kollman and S. Rothenberg, *J. Am. Chem. Soc.*, **99**, 1333 (1977).
(25) (a) S. Yamabe and K. Morokuma, *J. Am. Chem. Soc.*, **97**, 4458 (1975); (b) H. Umeyama, K. Morokuma, and S. Yamabe, *ibid.*, **99**, 330 (1977).

Importance of Electron Correlation in Computing Molecular Energies and Structures of Annulenes

H. Baumann

Contribution from the Laboratorium für Organische Chemie der Eidgenössischen Technischen Hochschule, 8092 Zürich, Switzerland. Received April 21, 1977

Abstract: In this work the failure of the MINDO methods in predicting correct geometries or enthalpies of formation (when geometries are known) in the case of the larger sized annulenes is studied. It is shown that one cause of this MINDO weakness could be the neglect of the correlation energy. The dependence of this energy on the size of the π system, the symmetry of the molecule, and the number of the considered doubly excited configurations are investigated. In the case of larger [4n + 2]annulenes, such as [14]- and [18]annulenes, the correlation energy is larger for geometries with π-bond delocalization than for those where π bonds are localized. For the larger [4n]annulenes this dependence on the degree of π-bond localization is less important. Some simple rules for estimating the importance of the correlation energy of π systems are given. The correlation effect like the singlet Hartree-Fock instability, to which it is related, is parameter dependent.

Introduction

Dewar et al.[1-4] have introduced different versions of MINDO programs that either compute the enthalpy of formation of an organic molecule of known geometry (MINDO/1) or allow for molecular optimization (MINDO/2 or MINDO/3). Serious failures of these MINDO methods have been reported.[5-9] For instance, Iwamura et al.[5] have shown that MINDO/2 completely fails to reproduce the correct heats of formation of the different C_8H_8 valence isomers, especially the strained ones. This inadequacy of MINDO/2 to account for strain energy associated with small rings has been corrected to a certain extent in the MINDO/3 version, as can be seen in Table I. In their investigation of [18]annulene using MINDO/3, Dewar et al.[10] reported that a planar structure with D_{3h} symmetry and localized π bonds is 108 kJ

mol^{-1} more stable than the D_{6h} structure with π bonds delocalized (see Table II). Although the computed enthalpy of formation is in very good agreement with the thermochemically determined enthalpy,[11] there remain well-founded doubts about these MINDO/3 results.[12] Cizek and Paldus[13] have reformulated the Hartree–Fock stability condition introduced by Thouless[14] (Appendix I). They treated all of the [4n + 2]annulenes of the maximum symmetry of D_{Nh} ($N = 4n + 2$) by PPP[15] using two parameter sets. With the "theoretical" set, delocalized [14]annulene is already HF unstable, whereas with the "Mataga" set, [22]annulene is the largest of the HF-stable annulenes. Toyota et al.[16] have repeated the PPP calculations with a "Mataga"-like parameter set but with optimization of the structures by bond-length variation and by starting with more realistic structures (Figure 2). They found similar results to those of Cizek et al.[13] for the lowest eigenvalues of the sta-